Sr_2Ni_3 – A Strontium Subnickelide?

Peter Höhn, Alexey Baranov, Stefan Hoffmann, Miroslav Kohout, Fabian Nitsche, Walter Schnelle, Frank R. Wagner, and Rüdiger Kniep

The chemistry of ternary and higher nitridometalates is a long-running research project at our institute [1,2]. In the previous scientific report we presented results on compounds in the system Sr-Ni-C-N [1]. To investigate the phase formation in this quaternary system pelletized mixtures of the elements and binary alkaline-earth nitrides were preferentially used. Our current investigations on the N species in these quaternary nitridometalates by use of ^{15}N-MAS-NMR spectroscopy necessitate the absolute absence of elemental Ni in the samples, a requirement not completely fulfilled by the current methods of synthesis. Therefore, alternate routes of preparation were investigated, one of them employing intermetallic compounds as starting materials.

The binary system Sr-Ni was first investigated in 1966 [3]. According to this study, SrNi is the only intermediate phase [4] (X-ray diffraction pattern indexed with a hexagonal unit cell, a = 332 pm, c = 701 pm [3]; no further structural information). Thus, SrNi might have been an ideal starting material for the synthesis of strontium nitridometalates.

From our first DTA experiments (Fig. 1) the existence of SrNi (melting point 860°C, incongruent, [3]) could not be confirmed. Instead, a new phase (Sr_2Ni_3, $P\overline{3}1m$ (Nr. 164), a = 412.617(1) pm, c = 868.567(1) pm) was obtained. In addition, the investigations did not give any evidence towards
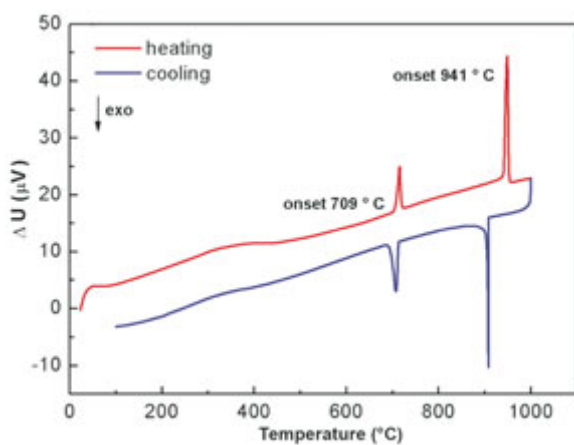

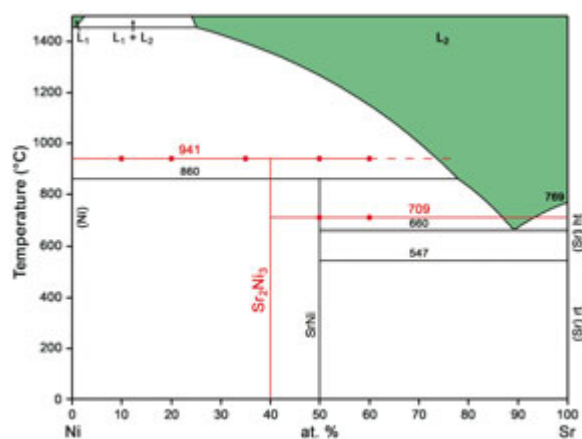*Fig. 1: Difference thermal analysis (DTA) of a sample of nominal composition SrNi.*

Fig. 2: The binary system Sr-Ni: Summary of literature data [3,4] and our preliminary results (red).

the existence of further intermediate phases in the binary system up to now. Literature data [3,4] as well as our preliminary results are summarized in figure 2.

For the preparation of Sr_2Ni_3 elemental strontium and nickel are mixed in the molar ratio 2:3, pelletized, sealed in a niobium tube under argon, and heated in a high-frequency furnace at 1300 °C for 10 minutes. Subsequent annealing at 600°C for 48 hrs results in single phase samples with a metallic luster. Microprobe investigations of a polished sample of nominal composition SrNi prepared in the same manner showed homogeneous regions with molar ratio Sr:Ni = 2:3 besides strontium-rich regions at the grain boundaries. DTA measurements yield 709 °C for the eutectic temperature and 941 °C for the peritectic decomposition of Sr_2Ni_3.

Sr_2Ni_3 is a metallic phase showing Pauli-paramagnetism. XAS investigations on Sr_2Ni_3 (Fig. 3) indicate a particular valence state for Ni, clearly different from characteristic Ni^0, Ni^I, or Ni^{II} states. Further discussions on the electronic structure of Sr_2Ni_3 are presented below.

The crystal structure of Sr_2Ni_3 ($P\overline{3}1m$ (Nr. 164), a = 412.617(1) pm, c = 868.567(1) pm, Fig. 4) was solved from synchrotron diffraction powder data and represents a new structure type.
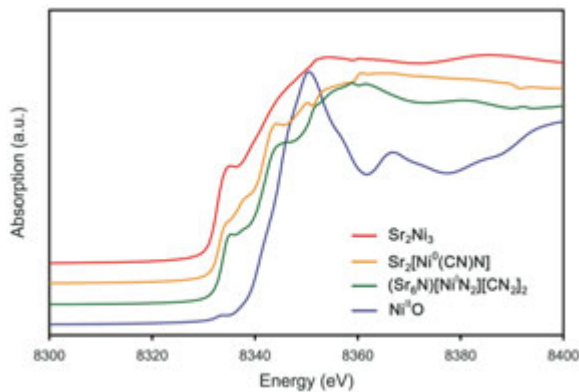
Fig. 3: X-ray absorption (XAS) spectra at the Ni K-edge of Sr_3Ni_2 and reference compounds containing Ni^0, Ni^I, and Ni^{II}, respectively.

The dominant structural motif consists of corrugated Ni layers (Fig. 5), which are separated along [001] by planar double layers of strontium. The degree of the corrugation corresponding to the displacement of Ni^t from $z = 0$ was determined as 36 pm. The designation Ni^o and Ni^t refers to the octahedral and tetrahedral strontium coordination of the nickel species within the respective voids of the *hcp* strontium arrangement. The complete coordination sphere around Ni^o is built up by 6 Sr and 6 Ni^t; Ni^t is surrounded by 3 Ni^o, 3 Ni^t and 4 Sr, whereas Sr features 3 Ni^o, 4 Ni^t and 9 Sr as nearest neighbors.

Distances Ni–Ni (241-249 pm) and Sr–Sr (413 pm within layers, 446 pm between layers) in Sr_2Ni_3 correspond well with values from the elements (Ni: 244 pm [5], Sr: 430 pm [6]); distances Sr-Ni range between 282 pm and 342 pm.

An alternate description of the crystal structure of Sr_2Ni_3 is based on the hexagonal close packed arrangement of the strontium atoms. The mode of occupation of tetrahedral and octahedral voids by nickel is schematically shown in Fig. 6 combined with related situations in other compounds.

The largest topological similarity with Sr_2Ni_3 is observed for Al_3Ni_2 [7]: both phases crystallize in the space group $P\bar{3}1m$ and are isopunctual without being strictly isotypic. The differences in the atomic positions are listed in Table 1.

Wyckoff	Sr_2Ni_3	Al_3Ni_2
2d	Sr, z = 0.7171(1)	Al, z = 0.648
1a	Ni^o	Al^o
2d	Ni^t, z = 0.0420(1)	Ni^t, z = 0.149

Table 1: Comparison of atomic positions in the crystal structures of Sr_2Ni_3 and Al_3Ni_2 [7].
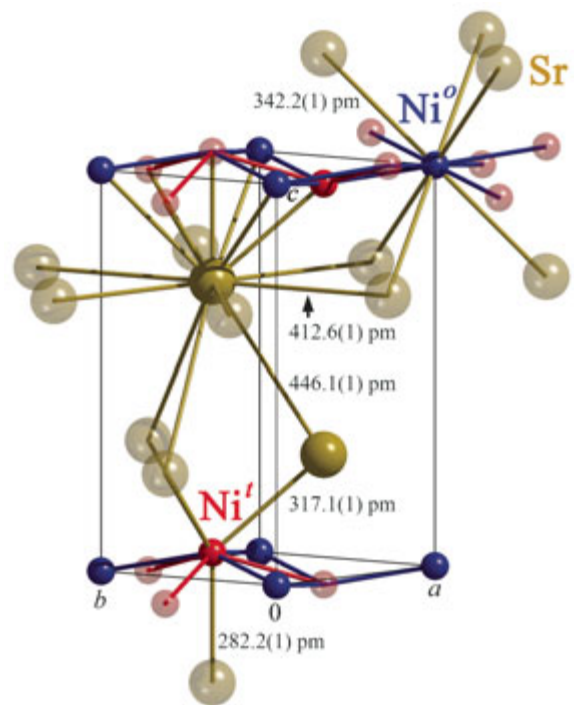

Fig. 4: Crystal structure of Sr_2Ni_3. Atoms located outside the unit cell are represented as transparent spheres. Tetrahedral and octahedral coordination of nickel by strontium (Ni^t and Ni^o, respectively) is emphasized.
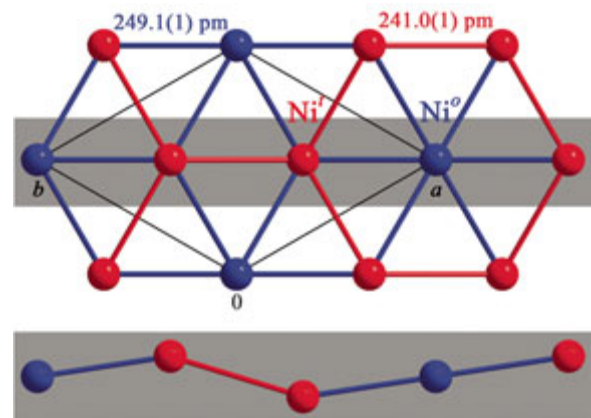

Fig. 5: Corrugated Ni layer in the crystal structure of Sr_2Ni_3, top: view along [001], bottom: side view of the section highlighted in grey.
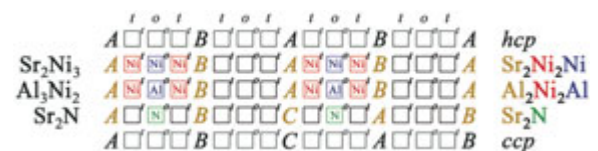

Fig. 6: Occupation of tetrahedral (t) and octahedral (o) voids in the crystal structures of Sr_2Ni_3, Al_3Ni_2, and Sr_2N, respectively. Empty voids are represented by □.

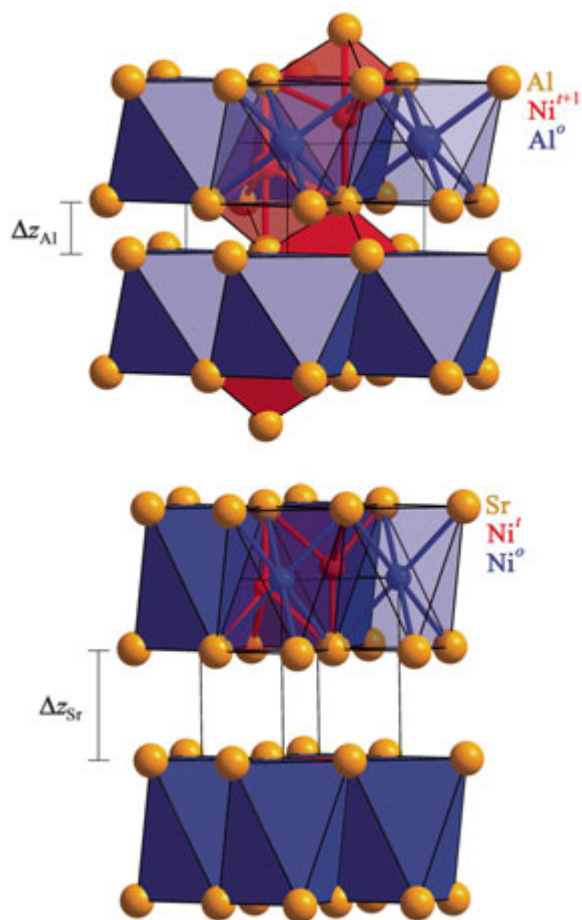*Fig. 7: Topological comparison of the crystal structures of Al_3Ni_2 (top) and Sr_2Ni_3 (bottom). Δz_x corresponds to the interlayer distance between filled double layers.*

Fig. 8: Topological comparison of the crystal structures of Sr_2Ni_3 (top) and Sr_2N (bottom).

As shown in Fig. 7, the distance between the double layers in Sr_2Ni_3 ($\Delta z_{Sr} = 0.434$) is considerably larger than in Al_3Ni_2 ($\Delta z_{Al} = 0.296$); the small interlayer distance (Δz_{Al}) of the occupied double layers in the crystal structure of Al_3Ni_2 leads to an enlargement of the coordination sphere of Ni in Al_3Ni_2 from tetrahedral to CN(Ni) = 5.

The electronic structure of Sr_2Ni_3 was calculated at the DFT/LDA level of theory employing the FPLO program system. A chemical bonding analysis has been carried out in position space on the basis of topological analyses (utilizing the program DGrid) of the electron density (Quantum theory of atoms in molecules, QTAIM method), which yields uniquely defined atomic regions, and on the basis of the electron localizability indicator ELI-D [8], leading to uniquely defined bonding regions. Due to the striking similarity of their crystal structures (Fig. 8), the results for Sr_2Ni_3 are compared with those of Sr_2N, which have already been published earlier [9].
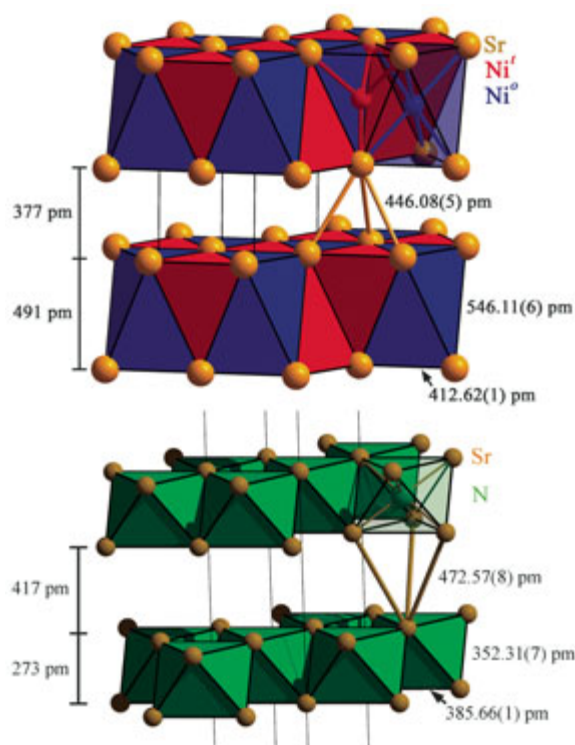
The Sr atoms given by the QTAIM method carry a positive charge of +0.8 and +1.2 for Sr_2Ni_3 and Sr_2N, respectively. Thus the Ni and the N atoms display the negative charges as expected from the electronegativity scale [10] ($EN_{Sr} = 0.95$, $EN_{Ni} = 1.91$, $EN_N = 3.04$). The volume demand of the Sr atoms is similar in both compounds with values of 36×10^6 pm^3 in Sr_2Ni_3 and 34×10^6 pm^3 in Sr_2N.

The QTAIM Sr atoms in Sr_2N form a double layer of mutually touching Sr QTAIM basins (Fig. 9 bottom). The QTAIM N atoms are found to be separated from each other. Similarly in Sr_2Ni_3 only the QTAIM Sr atoms of neighbouring double layers touch each other. Their contact in [001] direction is inhibited by the Ni layers. In these, the QTAIM basins of Ni^o species (green in Fig. 9 top) are only in contact with the Ni^t species (blue in Fig. 9 top).

The bonding for the peculiar inter-layer-type Sr–Sr contact was analyzed employing ELI-D (Fig. 10). The unification of the 1st to 4th shell ELI-D basin set yields the Sr core superbasin. The electronic populations (1.7 for both) for these superbasins are almost identical, and the sizes (Sr_2Ni_3: 14.7×10^6 pm^3 and Sr_2N: 16.5×10^6 pm^3) are very similar in Sr_2Ni_3 and Sr_2N. Inside the Sr–Sr inter-
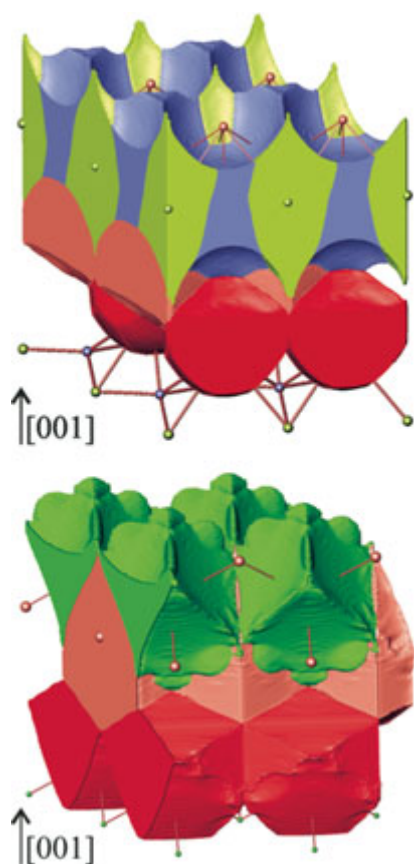
Fig. 9: QTAIM basins for Sr_2Ni_3 (top) and Sr_2N (bottom): Sr basins (red), N basins (green), Ni^o basins (pale green), Ni^t basins (blue).

layer region a band of higher localizability with ELI-D attractors is found in both compounds. While the volume demand of the corresponding basin sets is rather similar (Sr_2Ni_3: 37.8 × 10^6 pm³ and Sr_2N: 31.3 × 10^6 pm³) in both compounds, the electronic population is twice as large (Sr_2Ni_3: 1.4 e⁻, Sr_2N: 0.7 e⁻) in Sr_2Ni_3. This is due to the less ionic Sr–Ni bonding compared with Sr–N, which is also indicated by separate multicenter Sr–Ni bonding features (Fig. 10 top) visualized as separate 1.02-localization domains pointing from the Ni atoms towards the ELI-D attractors of the Sr interlayer band.

Taking into account the structural similarities, the physical properties and the electronic structure calculations, Sr_2Ni_3 may be regarded as a sub-nickelide in a similar sense as discussed for the subnitride Sr_2N [11], as well as for the mixed-valency subnitrides Sr_4N_3 [12] and $(Ca_7N_4)M_x$ [13]. From the point of view of electron counting and charge balancing of chemical formulae the subvalent state of the alkaline earth components in
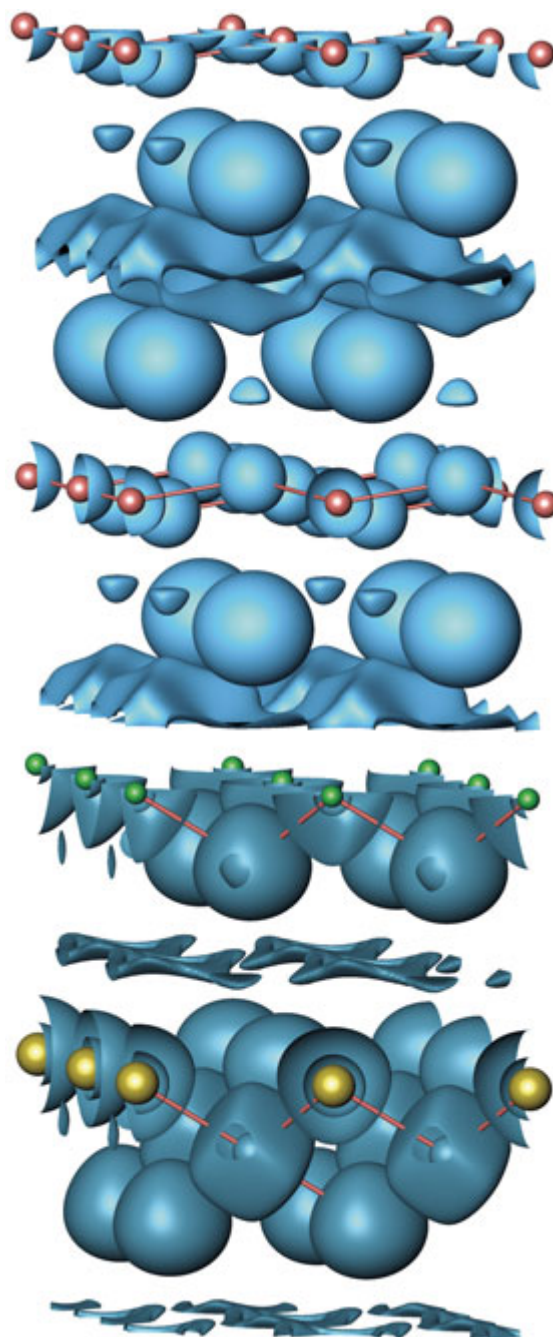

Fig. 10: ELI-D diagrams for Sr_2Ni_3 (top) and Sr_2N (bottom): Sr (yellow), Ni (red), N (green). Sr_2Ni_3: 1.02-localization domains of ELI-D display the interlayer Sr–Sr and a separate multicenter Ni–Sr bonding feature. Sr_2N: 1.12-localization domains of ELI-D displaying the interlayer Sr–Sr bonding.

these nitrides was best described as $AE^{1.5+}$. Applied to the intermetallic compound Sr_2Ni_3 this ionic picture would lead to $(Sr^{1.5+})_2(Ni^-)_3$. The significance of this mode of electron counting will also be a subject of our future research on this class of compounds.

References

[1]   *P. Höhn, M. Armbrüster, G. Auffermann, U. Burkhardt, F. Haarmann, A. Mehta, and R. Kniep,* in Scientific Report 2003-2005, p. 206 (Max Planck Institute for Chemical Physics of Solids, Dresden Germany, 2006).

[2]   *P. Höhn, J. Bendyna, W. Schnelle, and R. Kniep,* in Scientific Report 2006-2008, p. 153 (Max Planck Institute for Chemical Physics of Solids, Dresden Germany, 2009).

[3]   *Y. Takeuchi, K. Machizuki, M. Watanabe, and I. Obinata,* Metall **20** (1966) 2.

[4]   *H. Okamoto,* Binary Alloy Phase Diagrams, Second Edition, Ed. T.B. Massalski, ASM International, Materials Park, Ohio **3** (1990) 2865.

[5]   *A. W. Hull,* Phys. Rev. **10** (1917) 661.

[6]   *E. A. Sheldon and A. J. King,* Acta Crystallogr. **6** (1953) 100.

[7]   *A. J. Bradley and A. Taylor,* Phil. Mag. **23** (1937) 1049.

[8]   *M. Kohout,* Int. J. Quantum Chem. **97** (2004) 651. *M. Kohout,* Faraday Discuss. **135** (2007) 43. *F.R. Wagner, V. Bezugly, M. Kohout, and Yu. Grin,* Chem. Eur. J. **13** (2007) 5724.

[9]   *W. Bronger, R. Kniep, and M. Kohout,* Z. Anorg. Allg. Chem. **630** (2004) 117.

[10] *L. Pauling:* The nature of the chemical bond and the structure of molecules and crystals. Mei Ya Publications Taipei, 1960.

[11] *N. E. Brese and M. O'Keeffe,* J. Solid State Chem. **87** (1990) 134.

[12] *Y. Prots. G. Auffermann, M. Tovar, and R. Kniep,* Angew. Chem. Int. Ed. **41** (2002) 2288.

[13] *P. Höhn, G. Auffermann, R. Ramlau, H. Rosner, W. Schnelle, and R. Kniep,* Angew. Chem. Int. Ed. **45** (2006) 6681.